Journal of Neurology
https://doi.org/10.1007/s00415-023-12154-7

ORIGINAL COMMUNICATION

Cerebrospinal fluid NPTX2 changes and relationship with regional brain metabolism metrics across mild cognitive impairment due to Alzheimer's disease

Federico Massa[1,2] · Caterina Martinuzzo[1] · Nerea Gómez de San José[3] · Virginia Pelagotti[1] · Wendy Kreshpa[1] · Samir Abu-Rumeileh[4] · Lorenzo Barba[4] · Pietro Mattioli[1,2] · Beatrice Orso[1] · Andrea Brugnolo[1,2] · Nicola Girtler[1,2] · Tiziana Vigo[2] · Dario Arnaldi[1,2] · Carlo Serrati[5] · Antonio Uccelli[1,2] · Silvia Morbelli[2,6] · Andrea Chincarini[7] · Markus Otto[4] · Matteo Pardini[1,2]

Received: 8 November 2023 / Revised: 8 December 2023 / Accepted: 9 December 2023
© The Author(s), under exclusive licence to Springer-Verlag GmbH Germany 2023

Abstract

Background Neuronal pentraxin-2 (NPTX2), crucial for synaptic functioning, declines in cerebrospinal fluid (CSF) as cognition deteriorates. The variations of CSF NPTX2 across mild cognitive impairment (MCI) due to Alzheimer's disease (AD) and its association with brain metabolism remain elusive, albeit relevant for patient stratification and pathophysiological insights.

Methods We retrospectively analyzed 49 MCI-AD patients grouped by time until dementia (EMCI, $n=34$ progressing within 2 years; LMCI, $n=15$ progressing later/stable at follow-up). We analyzed demographic variables, cognitive status (MMSE score), and CSF NPTX2 levels using a commercial ELISA assay in EMCI, LMCI, and a control group of age-/sex-matched individuals with other non-dementing disorders (OND). Using [^{18}F]FDG PET scans for voxel-based analysis, we explored correlations between regional brain metabolism metrics and CSF NPTX2 levels in MCI-AD patients, accounting for age.

Results Baseline and follow-up MMSE scores were lower in LMCI than EMCI (p value $=0.006$ and $p<0.001$). EMCI exhibited significantly higher CSF NPTX2 values than both LMCI ($p=0.028$) and OND ($p=0.006$). We found a significant positive correlation between NPTX2 values and metabolism of bilateral precuneus in MCI-AD patients ($p<0.005$ at voxel level, $p<0.05$ with family-wise error correction at the cluster level).

Conclusions Higher CSF NPTX2 in EMCI compared to controls and LMCI suggests compensatory synaptic responses to initial AD pathology. Disease progression sees these mechanisms overwhelmed, lowering CSF NPTX2 approaching dementia. Positive CSF NPTX2 correlation with precuneus glucose metabolism links to AD-related metabolic changes across MCI course. These findings posit CSF NPTX2 as a promising biomarker for both AD staging and progression risk stratification.

Keywords Cerebrospinal fluid biomarkers · [^{18}F]FDG PET · Synaptic dysfunction · Mild cognitive impairment (MCI) · Alzheimer's disease · Neuronal pentraxin-2

✉ Federico Massa
fedemassa88@gmail.com

[1] Department of Neuroscience, Rehabilitation, Ophthalmology, Genetics, Maternal and Child Health (DINOGMI), University of Genoa, Genoa, Italy

[2] IRCCS Ospedale Policlinico San Martino, Genoa, Italy

[3] Department of Neurology, Ulm University Hospital, Ulm, Germany

[4] Department of Neurology, Martin-Luther-University Halle-Wittenberg, Halle (Saale), Germany

[5] Neurology Unit, ASL 1 Hospital, Imperia, Italy

[6] Department of Health Science (DISSAL), University of Genoa, Genoa, Italy

[7] National Institute of Nuclear Physics (INFN), Genoa Section, Genoa, Italy

Published online: 29 December 2023

Introduction

Significant progress has been made in understanding Alzheimer's disease (AD), uncovering molecular abnormalities and pathological changes detectable in cerebrospinal fluid (CSF). Alongside the well-established CSF biomarkers for amyloidosis (amyloid-β1-42, amyloid-β1-40, i.e., Aβ42/40 ratio), tauopathy (phosphorylated tau protein at threonine 181, p-Tau181), and neuronal death (total tau protein, t-Tau), additional markers could shed light on concurrent pathological events in AD. The early stages of AD are characterised by synaptic dysfunction and degeneration, which are strongly linked to the deposition of amyloid plaques and occur prior to neuronal loss, contributing to cognitive decline [1–4]. Therefore, researchers have targeted CSF biomarkers linked to synaptopathy, finding correlations with cognitive outcomes across disease stages [5, 6]. Belonging to the neuronal pentraxin family with NPTX1 and NPTXR, neuronal pentraxin-2 (NPTX2) fosters the development, maturation, and plasticity of synapses, particularly excitatory ones, thereby enhancing the proper functioning of neuronal circuits. Given its involvement in synaptic homeostasis, it has been proposed as a potential biomarker for synaptic dysfunction in neurodegenerative conditions like AD and frontotemporal lobar degeneration [7]. Understanding the variations of CSF NPTX2 levels across AD remains elusive, and evidence from different studies in CSF and brain tissue samples has been so far controversial. Various assay methods have consistently revealed lower levels of CSF NPTX2 in individuals with mild cognitive impairment (MCI), dementia, and even preclinical stages of AD, in comparison to healthy controls [8–13]. Furthermore, the magnitude of the decline in CSF NPTX2 concentrations was significantly higher in progressors than non-progressors to MCI or dementia [8, 11, 12]. Conversely, other authors have reported fluctuations in NPTX2 expression, with initial increases in mild-to-moderate stages followed by subsequent decreases in severe AD [14, 15]. Variations due to study design, sample size, disease stage, and assay techniques limit result generalizability. However, they consistently indicate changes in NPTX2 levels throughout the AD stages and highlight the potential of monitoring CSF NPTX2 to better understand synaptic degeneration and cognitive decline in AD.

The intricate AD pathophysiology, involving multiple molecular pathways, hampers precise NPTX2 variations comprehension. By integrating 2-deoxy-2-[^{18}F]fluoro-D-glucose PET ([^{18}F]FDG PET hereafter) imaging and CSF synaptic biomarkers, some studies have revealed metabolic associations of distinct proteins that undergo changes in distribution and relative significance during the AD course [6, 16, 17] However, to date, no study has delved into the metabolic correlates of CSF NPTX2 in prodromal AD.

To address this gap, our study analyzed individuals with MCI with a high likelihood of AD, stratified by progression rate to dementia within two years, indicative of disease stage. Our primary objective was to examine CSF NPTX2 variations in relation to AD dementia proximity. Additionally, we explored the correlation between CSF NPTX2 values and regional brain metabolism by [^{18}F]FDG PET imaging. This sought to unravel neurobiological variations and regions where the NPTX2-related synaptic alterations intersect with metabolic changes during disease progression.

Methods

Patients

We retrospectively selected a cohort of 49 patients (30 females; age 75.2 ± 5.3 (range 50.3–85.1); education 10.3 ± 4.4 years (range 5–23); MMSE score 26.6 ± 2.2 (range 21–30) with typical, high-likelihood MCI-AD, extracted from the database of 160 patients diagnosed with MCI-AD at the memory clinic of the University of Genoa (Italy, May 2017 to April 2021) based on the NIA-AA criteria [18]. Regarding the inclusion criteria, participants had undergone both lumbar puncture for CSF standard biomarkers (Aβ42, Aβ40, p-Tau181, and t-Tau), indicating an AD-compatible AT(N) profile [19], and [^{18}F]FDG PET scan within 2 months of each another. An indispensable requirement was a clinical follow-up lasting a minimum of 2 years.

At their first evaluation, participants were subjected to neurological, general medical examinations, and an extended battery of neuropsychological tests as described previously [17], which detailed an amnestic profile, either single or multidomain. All patients maintained preserved activities of daily living and instrumental activities of daily living, as confirmed through both clinical interviews and formal questionnaires. The Clinical Dementia Rating (CDR) scale was consistently at 0.5 for all patients, ultimately defining their condition as amnestic MCI [20]. Blood tests and brain magnetic resonance imaging (MRI) rule out non-degenerative causes of cognitive deficit.

Using a 2-year threshold, we divided the MCI-AD patients into two MCI stage subgroups. Unlike previous ADNI studies where patients were subdivided based on the extent of memory impairment [21, 22], we employed a temporal criterion for proximity to dementia conversion, similar to our earlier study [17]. We designated late-MCI patients (LMCI, $n = 15$) if progressing to dementia within 2 years from baseline (1.4 ± 0.3 years) and early-MCI patients (EMCI, $n = 34$) if they progressed after 2 years or remained stable at the MCI level during follow-up (3.0 ± 0.8 years, range 2.1–4.8). Dementia progression was determined by

a CDR score of 1 in clinical interview with patients and relatives.

Control groups

For [^{18}F]FDG PET comparisons, we included a healthy control (HC) group made up of 40 age-, sex- and education-matched volunteers, previously described [17]. For CSF biomarker comparisons, we added a second group of 43 age- and sex-matched individuals with other non-dementing (OND) conditions who had undergone CSF analysis for diagnostic purpose. This group included 18 patients having normal pressure hydrocephalus, 9 cerebrovascular disease, 7 amyotrophic lateral sclerosis without cognitive impairment, 4 inflammatory disease of either peripheral or central nervous system, 3 worried-well patients without cognitive disorder post-extensive diagnostic workup, and 2 healthy subjects performing lumbar puncture for orthopaedic surgery. Their cognitive status was checked with an MMSE score > 27 and CDR = 0, and they had normal CSF Aβ42/Aβ40 ratio, p-Tau181, and t-Tau values.

CSF biomarkers

CSF collection and pre-processing followed the standard operating procedures (details in Supplementary methods). We utilized the Lumipulse G600 II® fully automated chemiluminescent enzyme immunoassay system (Fujirebio Europe, Gent, Belgium) to measure CSF AD standard biomarkers (Aβ42, Aβ40, p-Tau181, and t-Tau) in both MCI-AD and OND individuals. Assay cartridge datasheet cut-offs were also verified in our center: Aβ42/40 ratio 0.069, p-Tau181 56.5 pg/mL, t-Tau 404 pg/mL [17]. Using the same samples, we quantified i) NPTX2 with commercially available ELISA assay (INNOTEST, Fujirebio Europe, Gent, Belgium), and ii) NfL through Simple Plex™ Ella™ automated microfluidic platform (ProteinSimple). Protein concentrations were measured in pg/mL. Intra-test reproducibility had an average coefficient of variation (CV) below 10%, and inter-test reproducibility averaged below 15% for all assays.

[^{18}F]FDG PET imaging protocol

The methodology for acquisition and image pre-processing is described in prior research [17] and Supplementary methods.

Voxel-based analysis (VBA)

Pre-processed images were subjected to whole-brain voxel-wise group analyses, namely:

(1) The comparison between MCI-AD and HC groups (two-sample t-test; nuisance: age) to identify AD-related hypometabolic regions (i.e., a disease pattern);
(2) The comparison between EMCI and LMCI patients (two-sample t-test; nuisance: age) to obtain a 'progression' pattern, including those regions with different brain metabolism as MCI progresses from its early to later stages;
(3) Linear correlation analysis between the brain metabolism and CSF levels of NPTX2 in MCI-AD patients (multiple regression, nuisance: age).

We used a 0.8 grey matter threshold mask and normalized raw values based on cerebellar cortex activity. We applied $p < 0.001$ voxel-level height threshold without multiple comparison correction.

From the resulting SPM t-Map, we considered those ≥ 100-voxel clusters, significant at $p < 0.05$ FWE-corrected for multiple comparisons at cluster-level. Cluster coordinates were converted using Ginger Ale and Talairach Client software for mapping onto the Brodmann-classified Talairach 3D atlas.

Volumes of interest (VOI)-analysis

VOIs included significant clusters from (i) MCI-AD vs. HC comparison (disease-related-VOI, DIS-VOI), (ii) EMCI vs. LMCI comparison (progression-related-VOI, PROG-VOI), (iii) CSF NPTX2 correlation with brain metabolism (NPTX2-VOI). Using the Marsbar toolbox for SPM, we computed the average count density of each VOI in every subject, then scaled against cerebellar cortex mean count as reference.

Statistics

Demographic–clinical data comparison between EMCI and LMCI used unpaired two-tailed T-test or Wilcoxon rank-sum test if needed, FDR-corrected for multiple comparisons. Categorical variables employed Fisher's exact test. CSF biomarker levels in EMCI, LMCI, OND groups were examined through Mann–Whitney *U* Test with Bonferroni-corrected post hoc comparisons. Outliers detected via Robust regression and Outlier removal (ROUT) method (Q < 1%) were excluded.

CSF biomarker values, including MCI-AD and OND, were correlated using Spearman's test. Due to right-skewed CSF NPTX2 distribution (Lilliefors test, $p < 0.0001$), logarithmic (log-) transformation was applied for more symmetric distribution enabling linear correlations with brain metabolism in VBA and VOI-analyses. In the latter, we correlated the cerebellum-scaled mean count density of the NPTX2-VOI with the log-NPTX2 values by Spearman's

test considering either i) the entire MCI-AD group or ii) the EMCI and LMCI, separately. Supplementary analysis extended similar correlations of log-NPTX2 values with either DIS-VOI or PROG-VOI counts.

Statistical analysis utilized GraphPad Prism version 9 (GraphPad Software, San Diego, California, USA), with $p < 0.05$ significance threshold.

Results

Clinical and CSF biomarker data

Table 1 summarizes main clinical–demographic features and CSF biomarker values for MCI-AD patients. Briefly, LMCI had lower MMSE at baseline (MMSE-BS) and follow-up (MMSE-FU) than EMCI ($p^{FDR} = 0.006$ and $p^{FDR} < 0.001$, respectively), while ΔMMSE (MMSE-FU *minus* MMSE-BS) was higher in LMCI than EMCI ($p^{FDR} < 0.001$). These findings indicate more significant cognitive impairment and progressive decline in later stage MCI.

CSF AD standard biomarkers differed in EMCI and LMCI compared with OND ($p < 0.001$) as expected, but not one with another. A trend of elevated CSF NPTX2 in entire MCI-AD cohort vs. OND was observed ($p = 0.054$, Fig. 1A). CSF NPTX2 differed among groups ($p = 0.003$); post hoc analysis showed EMCI had higher values than LMCI ($p = 0.028$) and OND ($p = 0.006$) (Table 1, Fig. 1B).

Voxel-based analysis (VBA)

MCI-AD vs. HC group (DIS-VOI)

Two significant hypometabolism clusters (AD1-VOI and AD2-VOI) were found in MCI-AD vs. HC, forming DIS-VOI. These clusters covered bilateral precuneus/posterior cingulate (PC/PCC), left fusiform, superior and middle temporal, and supramarginal gyri (Fig. 2A).

Table 1 Main clinical characteristics and CSF biomarkers levels in/of MCI-AD patients

Demographical and clinical variables	MCI-AD ($n = 49$)	EMCI ($n = 34$)	LMCI ($n = 15$)		p value[#]	p^{FDR}-value*
Age (years)	75.2 ± 5.3	74.6 ± 4.1	76.6 ± 7.2		0.09	0.07
Sex (M:F)	19:30	15:19	4:11		0.34[§]	
Education	10.3 ± 4.4	10.8 ± 4.0	9.3 ± 5.1		0.14	0.08
MMSE score (BS)	26.6 ± 2.2	27.2 ± 1.9	25.2 ± 2.5		**0.006**	**0.006**
MMSE score (FU)	23.3 ± 3.9	25.3 ± 2.7	19.0 ± 2.1		**< 0.001**	**< 0.001**
Δ MMSE	3.3 ± 3.1	1.9 ± 2.5	6.2 ± 2.0		**< 0.001**	**< 0.001**
CSF biomarkers	MCI-AD ($n = 49$)	EMCI ($n = 34$)	LMCI ($n = 15$)	OND ($n = 43$)	p value[¶]	Post-hoc comparisons[‡]
Aβ42/Aβ40 ratio	0.045 ± 0.01	0.044 ± 0.010	0.048 ± 0.010	0.097 ± 0.012	**< 0.0001**	LMCI < OND $p < 0.0001$ EMCI < OND $p < 0.0001$
p-Tau181 (pg/ml)	111.9 ± 63.3	116.3 ± 70.9	102.0 ± 41.3	26.2 ± 9.15	**< 0.0001**	LMCI > OND $p < 0.0001$ EMCI > OND $p < 0.0001$
t-Tau (pg/ml)	737.6 ± 384.2	761.9 ± 420.0	682.5 ± 292.3	233 ± 106	**< 0.0001**	LMCI > OND $p < 0.0001$ EMCI > OND $p < 0.0001$
NPTX2 (pg/ml)	1049.3 ± 558.4	1093 ± 488	824.4 ± 445	783.0 ± 417.0	**0.003**	EMCI > LMCI $p = 0.028$ EMCI > OND $p = 0.006$
NfL (pg/ml)	1332.5 ± 652.2	1320.0 ± 560	1360.7 ± 847.9	1528 ± 869	0.76	

[§]p values for Fisher's exact test

[#]p values for Wilcoxon rank-sum test

*False discovery rate (FDR) adjusted p-value

[¶]p values for Mann-Witney test

[‡]p values for Bonferroni post-hoc test

Mean ± SD are shown. Significant values are in bold

MCI-AD Mild cognitive impairment due to Alzheimer's disease, *EMCI* Early mild cognitive impairment, *LMCI* Late mild cognitive impairment, *F* female, *M* male, *MMSE* Mini Mental State Examination, *BS* Baseline, *FU* Follow-up, *CSF* Cerebrospinal fluid, *Aβ42/Aβ40 ratio* amyloid Aβ1-42 normalized for amyloid Aβ1-40, *pTau181* Tau phosphorylated at threonine 181, *t-Tau* total Tau, *NPTX2* Neuronal Pentraxin 2, *NfL* neurofilament light chain

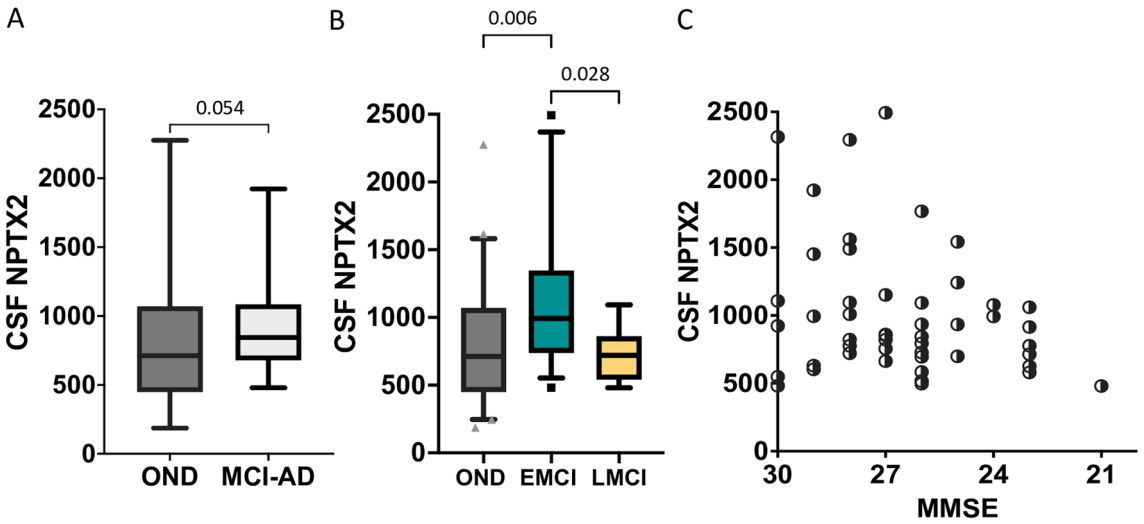

Fig. 1 Comparisons of cerebrospinal fluid (CSF) NPTX2 values (in pg/ml) of: 1A) individuals in the OND and MCI-AD groups (grey and white box plots respectively), and 1B) EMCI, LMCI, and OND groups (depicted by grey, green, and orange box plots respectively). The box plots illustrate the median concentration, the 25th and 75th percentiles, and the whiskers indicate the 5% to 95% confidence interval. Any statistically significant p-values are displayed as numbers. In Fig. 1C the scatter plot indicates the relationship between CSF NPTX2 levels (pg/ml, Y-axis) and MMSE score at baseline (X-axis, ranging from 21 to 30 points). The values are represented visually using half-black and half-white circles, illustrating a unique distribution where higher NPTX2 values align with higher MMSE scores, indicating lower levels of cognitive impairment. These values progressively decrease in conjunction with the MMSE scores, reflecting the progression towards dementia. Abbreviations: *MCI-AD* mild cognitive impairment due to Alzheimer's disease, *EMCI* early M, *LMCI* late MCI, *OND* other non-dementing disorders

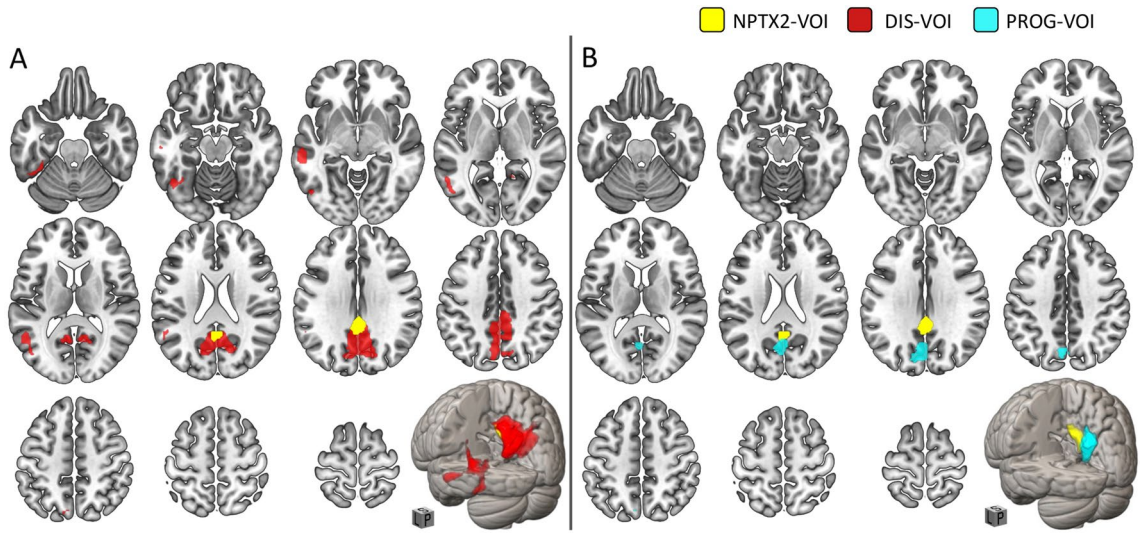

Fig. 2 The two-dimensional representation (axial cuts) and three-dimensional rendering show the metabolic correlate of NPTX2 (NPTX2-VOI) in yellow superimposed on the MNI reference atlas (using MRIcroGL software, https://www.nitrc.org/projects/mricrogl). Its spatial overlap can be evaluated in relation to A) the DIS-VOI (in red), derived from the comparison between MCI-AD and HC groups, or B) the PROG-VOI (in light blue), derived from the comparison between EMCI and LMCI patients. In the 3D rendering, mid-line sagittal and coronal cuts were used to enhance the visualization of the VOIs. Abbreviations: *VOI* volume of interest, *DIS-VOI* disease-related VOI, *PROG-VOI* progression-related-VOI, *L* left, *R* right, *P* posterior, *S* superior. Others as in Fig. 1

EMCI *vs.* LMCI (PROG-VOI)

We showed a significant relative hypometabolism in LMCI patients compared to EMCI patients in the left precuneus and posterior cingulate cortex (Fig. 2B).

Metabolic correlates of log-NPTX2 in MCI-AD patients

A significant positive correlation was demonstrated between log-NPTX2 values and metabolic levels in bilateral precuneus (Fig. 2A–B). Table 2 provides details on cluster extent, coordinates, and corresponding Brodmann areas for the mentioned VOIs.

VOI analysis

We observed a significant positive correlation between cerebellum-scaled mean count density of NPTX2-VOI and log-NPTX2 values for the entire MCI-AD group ($p < 0.001$, $r = 0.55$). This association was stronger in the EMCI subgroup ($p < 0.0001$, $r = 0.62$), but not significant in the LMCI group ($p = 0.29$, $r = 0.15$), separately (Fig. 3).

Additionally, a significant positive correlation existed between cerebellum-scaled mean count density of DIS-VOI and log-NPTX2 values for the entire MCI-AD group ($p = 0.006$, $r = 0.36$). This correlation was primarily driven by the EMCI subgroup ($p = 0.02$, $r = 0.35$) and was not significant in the LMCI group alone ($p = 0.28$, $r = 0.16$) (supplementary Fig. 2 s A–C).

Lastly, a significant positive correlation emerged between cerebellum-scaled mean count density of PROG-VOI and log-NPTX2 values for the entire MCI-AD group ($p = 0.02$,

Table 2 Significant brain areas resulting from the VBA of [18F]FDG PET scans

Cluster extent	Cluster significance	Cluster peaks coordinates			Cortical region (gyrus)	BA
		x	*y*	*z*		
Hypometabolism in MCI-AD with respect to HC group (DIS-VOI)						
3093	$p < 0.05$ FWE corr	− 5,11	− 53,97	18,9	Left posterior cingulate	30
(AD1-VOI)		− 7,12	− 69,74	26,38	Left precuneus	31
		4,15	− 50,29	19,4	Right posterior cingulate	30
		4,09	− 47,09	25,11	Right posterior cingulate	23
		7,69	− 69,81	26,62	Right precuneus	31
		13,1	− 78,17	34,93	Right cuneus	19
688	$p < 0.05$ FWE corr	− 47,25	− 56,03	− 16,24	Left fusiform gyrus	37
(AD2-VOI)		− 47,28	− 59,93	− 14,81	Left fusiform gyrus	37
		− 49,47	− 56,94	12,46	Left middle temporal gyrus	39
		− 56,51	− 32,28	− 8,75	Left middle temporal gyrus	21
		− 53,24	− 57,45	17,75	Left superior temporal gyrus	22
		− 37,95	− 50,31	− 17,35	Left fusiform gyrus	37
		− 43,97	− 68,33	13,28	Left middle temporal gyrus	39
		− 53,02	− 59,43	− 0,45	Left middle temporal gyrus	37
		− 51,4	− 52,04	20,1	Left supramarginal gyrus	40
		− 56,63	− 42,29	− 2,49	Left middle temporal gyrus	21
		− 53,37	− 52,9	28,99	Left supramarginal gyrus	40
		− 54,84	− 48,24	0,58	Left middle temporal gyrus	22
Hypometabolism in EMCI vs. LMCI patients (PROG-VOI)						
723	$p < 0.05$ FWE corr	− 5,28	− 73,47	26,05	Left precuneus	31
		− 1,39	− 62,96	14,5	Left posterior cingulate	23
Correlation with neuronal pentraxin-2 levels (NPTX2-VOI)						
364	$p < 0.05$ FWE corr	− 3,33	− 43,5	27,13	Left precuneus	31
		2,23	− 34,38	29,88	Right precuneus	31
		− 3,34	− 32,67	31,75	Left precuneus	31

Peak coordinates and cortical regions in each cluster are ordered downwards from the highest peak *Z* score

BA Brodmann area, *HC* healthy controls, *MCI-AD* Mild cognitive impairment due to Alzheimer's disease, *EMCI* Early mild cognitive impairment, *LMCI* Late mild cognitive impairment, *VOI* volumes of interest, *DIS-VOI* disease-related-VOI, *PROG-VOI* progression-related VOI, *NPTX2* neuronal pentraxin-2

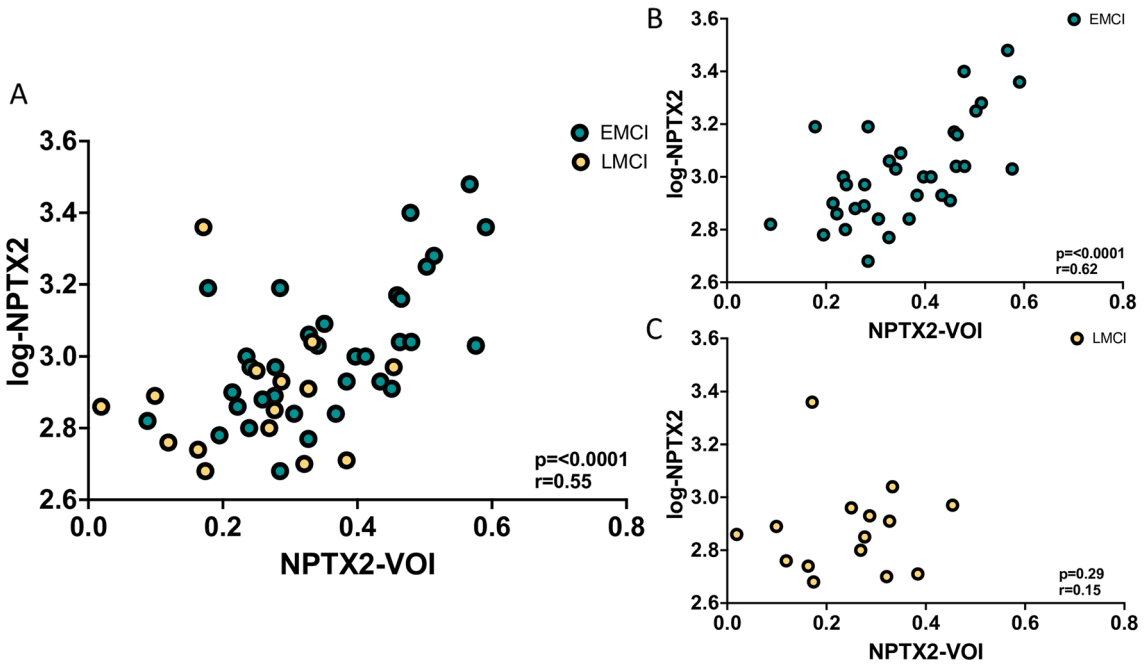

Fig. 3 Scatter plot of the cerebellum-scaled mean count density of the NPTX2-VOI (x-axis) and the log-NPTX2 values (y-axis) in the whole MCI-AD samples (3**A**) and in EMCI (3**B**) and LMCI (3**C**), separately. EMCI and LMCI patients are visually represented as round circles, with EMCI depicted as green circles and LMCI as orange circles. Spearman's rank-order correlation coefficient (r) and *p* values are displayed in the down-right corner

$r = 0.29$). However, this correlation was not significant in separate EMCI and LMCI analyses ($p = 0.12$, $r = 0.20$ and $p = 0.20$, $r = 0.23$, respectively) (supplementary Fig. 2 s D–F).

CSF biomarker correlations

In the entire subject sample, we found significant positive correlations between CSF levels of NPTX2 and p-Tau181 ($p = 0.009$, $r = 0.29$) as well as t-Tau ($p = 0.007$, $r = 0.29$), and a negative correlation with Aβ42/40 ratio ($p = 0.005$, $r = -0.30$). As expected, p-Tau181 and t-Tau exhibited an excellent positive correlation ($p < 0.0001$, $r = 0.94$), and each had a strong negative correlation with Aβ42/40 ($p < 0.0001$, $r = -0.76$ and $r = -0.73$, respectively) (Supplementary Fig. 1 s).

Discussion

The present findings support the role of CSF NPTX2 as a potential indicator for synaptic alterations associated with clinical progression within the AD continuum.

We observed that individuals in the early MCI stage exhibited significantly higher levels of CSF NPTX2 compared to either control subjects or those patients with MCI in a later stage nearing dementia progression based on a 2-year threshold. This paralleled the variations in cognitive performance, as evidenced by MMSE scores at baseline and follow-up. It should be acknowledged that the categorization into EMCI and LMCI may be less precise when considering the duration of MCI, which, however, is a highly variable and unreliable measure in degenerative diseases where a clear index event is lacking. Nevertheless, this categorization, drawn from prior works on the ADNI database [21, 22], highlighted differences in both cognitive severity and rate of progression to dementia potentially indicate distinct stages of neuropathological severity.

Previous studies have consistently reported lower levels of NPTX2 in individuals with AD-related dementia compared to healthy controls. Significant downregulation of NPTX2 was observed in the neuropathological study by Sathe et al. (2021) [9] considering AD patients with moderate-to-severe neurofibrillary tangle pathology and frequent neuritic plaques. In other mass spectrometry studies, the most significant declines in CSF NPTX2 concentrations were in individuals with MCI nearing dementia [8, 12], in demented patients with AD pathology (A + T +) compared to controls[14] and, more recently, in cognitively normal participants developing MCI more rapidly [12]. Likewise, employing ELISA assays, different researchers reported that levels of CSF NPTX2 paralleled cognitive impairment, being lower in MCI patients than controls [13, 23, 24].

The peculiar changes of CSF NPTX2 observed in our study across MCI can be explained by the homogenous biological characteristics of the patient cohort. Indeed, we strictly included patients being A + T + according to the AT(N) research framework for AD [19]. Conversely, the abovementioned studies using ELISA assay [13, 23, 24] based on a clinical AD diagnosis [18] and might have included other aetiologies in absence of amyloidosis biomarker data. Moreover, categorizing the MCI group based on progression time towards dementia allowed us to specifically examine an early MCI stage, revealing elevated CSF NPTX2 levels. This observation aligns with the study by Watson et al.(2023) [14] where CSF NPTX2 concentrations were higher in cognitively normal patients within the AD spectrum (A + T +) compared to healthy controls and enabled accurate differentiation between symptomatic and asymptomatic patients. Similarly, Perna et al. (2021) [15] noted heightened NPTX2 expression in the entorhinal cortex among mild-to-moderate AD patients, followed by a decline in severe AD cases.

The NPTX2 changes across MCI stages in our study, despite stable AT(N) biomarkers (including NfL), align with the dynamic model proposed by Sperling et al. (2011) [2]. This suggested early MCI shows pronounced synaptic dysfunction linked to cognitive decline, while other AD-related changes exhibit fewer substantial alterations through MCI. This suggests synaptopathy biomarkers may better capture MCI stages compared to AD pathology or neurodegeneration biomarkers.

Changes in NPTX2 levels may stem from diverse mechanisms. Increased levels during early MCI might indicate enhanced gene expression or synaptic enlargement by relatively unaffected neurons, countering amyloid and neurofibrillary tangle-induced damage [25–28]. However, disease advancement could overwhelm compensatory efforts, impacting protein production, including NPTX2, and leading to reduced CSF levels in later stages [10]. Aligned with the concept of NPTX2 as an early AD resilience factor, heightened baseline CSF NPTX2 levels correlated with increased p-tau181 and t-tau levels in preclinical individuals in a recent mass spectrometry study. An accelerated NPTX2 decline over time was also noted, potentially reflecting progressive neuronal and/or synaptic loss [12].

By interpreting the modest correlation between CSF NPTX2 levels and amyloidosis or tauopathy indicators in our study, we hypothesize additional mechanisms beyond the amyloid cascade may impact synaptic response. Early microglial activation and neuroinflammation may promote neuroprotection and compensatory synaptic responses, including NPTX2 production. In later stages, chronic pro-inflammatory status disrupts synaptic and neuronal regulation, gradually reducing CSF NPTX2 [31]. Moreover, due to structural similarity to pentraxins, linked to immune response and complement activation, NPTX2 level variations may affect debris clearance and complement/microglial-mediated synaptic pruning, ultimately exacerbating disease progression [29–31].

In the present study, we have integrated CSF NPTX2 and [^{18}F]FDG PET assessments, the latter serving as a sensitive metric for AD-related downstream neurodegeneration [32], as well as synaptic and neuronal-astrocyte activity, network disruption, and deafferentation [33–36]. Preliminarily, we log-transformed CSF NPTX2 values to approximate symmetrical distribution and facilitate linear analysis, consistent with prior research on synaptic biomarkers in MCI and AD [26]. Additionally, we normalized raw metabolic values using cerebellar cortex activity, not whole brain counts, which suits neurodegenerative conditions like AD, leveraging the unaffected cerebellum to enhance cortical abnormality detection [37]. We observed a significant positive correlation between log-NPTX2 levels and glucose metabolism in the bilateral precuneus (NPTX2-VOI), notably strongest in the EMCI group based on subsequent VOI-analysis. This NPTX2-VOI was within a broader hypometabolic area obtained from MCI-AD patients versus HC group comparison (DIS-VOI), encompassing bilateral precuneus/posterior cingulate cortex, left temporal, and parietal regions. Additionally, the NPTX2-VOI spatially overlapped with the region distinguishing EMCI from LMCI (PROG-VOI), signifying disease progression and extending into the left posterior cingulate cortex. In AD, altered glucose metabolism and connectivity in the precuneus are early indicators of cognitive decline and AD progression [38]. Hence, elevated CSF NPTX2 levels were associated with relatively preserved precuneus metabolism during early MCI, declining alongside precuneus impairment as MCI advanced. This reveals an intertwined relationship between CSF NPTX2 and precuneus metabolism, particularly in early MCI, yielding valuable insights into the progression of synaptic alterations toward dementia.

We noted a mild correlation between CSF NPTX2 levels and values in DIS-VOI and PROG-VOI, with a slightly stronger association observed in DIS-VOI. This suggests that CSF NPTX2 changes could reflect both inherent metabolic shifts seen in AD and the progression of metabolic decline in MCI. Notably, these correlations were weaker (NPTX2-VOI, DIS-VOI) or lost significance (PROG-VOI) when examining LMCI separately. While limited LMCI sample size hampers definitive conclusions, it is plausible that advanced MCI stages involve additional mechanisms beyond synaptic changes influencing glucose metabolism in specific regions. In contrast, in EMCI, [^{18}F]FDG PET signals may primarily denote synaptic modifications in posterior temporo-parietal cortex, reflecting progressive deafferentation from entorhinal–hippocampal region, an area affected early in AD [38].

Our study provides novel insights by revealing a correlation between glucose metabolism in a specific AD-related region and CSF NPTX2 in MCI-AD individuals. This extends our previous findings which emphasized unique metabolic correlations associated with specific synaptic proteins [17]. Specifically, we observed a negative correlation of CSF neurogranin and α-synuclein with metabolic changes in left precuneus/posterior cingulate cortex and of CSF β-synuclein with those in left lateral temporal regions. Other researchers found a positive correlation of CSF neurogranin and Growth-Associated Protein 43 (GAP-43) levels with glucose metabolism in temporal and angular regions [6]. Noteworthy, they employed standardized uptake value ratio (SUVr) analysis of predefined composite regions of interest (meta-ROIs) covering common affected regions in MCI-AD, whereas our study utilized voxel-wise correlation analysis without predefined regions. Furthermore, another study employed surface-based analysis of [^{18}F]FDG PET scans and found a positive correlation of CSF NPTX2 levels with reduced glucose metabolism in the temporal and parietal cortices of individuals with Down Syndrome and co-existing AD at varying stages [39]. However, the differences in the methodology and target population hinder direct comparisons with our results.

It is necessary to acknowledge the limitations of this study, including its retrospective nature and the relatively small sample size, although mirroring the real-world clinical scenario in terms of demographical variables. The careful selection of patients with a high-likelihood AD [18], partially compensates for this latter limitation, which is mostly due to the unconventional [^{18}F]FDG PET and CSF biomarker pairing in clinical context. Importantly, [18F]FDG PET is routinely combined with CSF analysis in our center for all subjects with amnestic MCI and a neurochemical profile compatible with AD. This approach provides additional insights into metabolism changes within the research framework, while the use of both biomarkers was not primarily attributed to an unusual disease course or a more complex diagnosis.

The absence of overt AD dementia is further explained by the challenges in conducting both [^{18}F]FDG PET and CSF biomarkers at this disease stage. Larger cohorts across AD stages are needed to validate findings, and longitudinal studies could offer insights into CSF NPTX2 trajectory. In fact, actual within-subject changes in the time-course of MCI towards AD are not discernible from our cross-sectional study, lacking multiple time points of observation. However, by stratifying patients based on the different time of progression to dementia and cognitive levels, as emphasized by the difference in MMSE scores, two distinct stages in the MCI course where NPTX2 levels exhibit significant differences become apparent.

Expanding data to include more synaptic proteins would aid establishing a fingerprint of synaptic dysfunction in the early phases of disease. This would serve prognostic purposes in the clinical setting and guide precise therapeutic trial patient selection.

Conclusions

Our study provides insights into the CSF NPTX2 variations and correlation with brain metabolism metrics in a pivotal area for cognitive functioning across MCI with AD etiology. In this context, NPTX2 emerges as a promising biomarker for disease staging and stratifying risk of progression toward dementia in the short-to-medium term.

Author contributors

Study concept and design of the work: FM, DA, PM, BO, AB, NG, SM, AC, MP; data acquisition, analysis, or interpretation: FM, CM, VP, NG, WK, SA, LB, TV, DA, CS, AU, MO, AC, SM, MP; drafting the manuscript: FM, CM, MP. All the authors participated in the critical revision and final approval of the manuscript to be published. FM guarantees for the overall content.

Supplementary Information The online version contains supplementary material available at https://doi.org/10.1007/s00415-023-12154-7.

Acknowledgements This work was developed within the framework of the DINOGMI Department of Excellence of MIUR 2018-2022 (legge 232 del 2016). The authors are thankful to Davide Visigalli for his technical assistance in the sample pre-analysis and biobanking work.

Funding This work was partially supported by a grant from the Italian Ministry of Health to IRCCS Ospedale Policlinico San Martino [Fondi per la Ricerca Corrente, and Italian Neuroscience network (RIN)], by #NEXTGENERATIONEU (NGEU) and partially funded by the Ministry of University and Research (MUR), National Recovery and Resilience Plan (NRRP), project MNESYS (PE0000006)—A Multiscale integrated approach to the study of the nervous system in health and disease (DN. 1553 11.10.2022).

Data availability Data are available on reasonable request from the corresponding author.

Declarations

Conflict of interest F Massa has received speaker honorarium from Roche Diagnostic Spa, Gómez de San José N is a part-time employer at Proteintech, S Abu-Rumeileh S received research support from the Medical Faculty of Martin-Luther-University Halle-Wittenberg (Clinician Scientist-Program No. CS22/06), D Arnaldi received fees from Fidia, Bruno, Italfarmaco, Idorsia for lectures and board participation; A Uccelli, received grants (to his Institution) from FISM, Biogen, Roche, Alexion, Merck Serono; participated on a Data Safety Monitoring Board or Advisory Board (to his Institution) for BD, Biogen, Iqvia, Sanofi, Roche, Alexion, Bristol Myers Squibb; S Morbelli has received

speaker Honoraria from G.E. Healthcare; Otto M received fees for advisory board meetings from Roche, Biogen, Grifols, and Axon; M Pardini receives research support from Novartis and Nutricia, received fees from Novartis, Merck. The other authors have nothing to disclose.

Informed consent and consent to publish This research involves human participants and was approved by the regional ethical committee (ref:PNRR-POC-2022–12376726). Informed consent was obtained from all participants. Anonymized data published per hospital rules for retrospective data collected during the clinical routine. All procedures followed the 1964 Helsinki Declaration and its later amendments.

References

1. Colom-Cadena M, Spires-Jones T, Zetterberg H, Blennow K, Caggiano A, DeKosky ST, Fillit H, Harrison JE, Schneider LS, Scheltens P, de Haan W, Grundman M, van Dyck CH, Izzo NJ, Catalano SM (2020) Synaptic Health Endpoints Working Group. The clinical promise of biomarkers of synapse damage or loss in Alzheimer's disease. Alzheimers Res Ther 12(1):21. https://doi.org/10.1186/s13195-020-00588-4. PMID: 32122400; PMCID: PMC7053087
2. Sperling RA, Aisen PS, Beckett LA et al (2011) Toward defining the preclinical stages of Alzheimer's disease: Recommendations from the National Institute on Aging-Alzheimer's Association workgroups on diagnostic guidelines for Alzheimer's disease. Alzheimer's Dementia 7:280–292. https://doi.org/10.1016/j.jalz.2011.03.003
3. Lleó A, Núñez-Llaves R, Alcolea D et al (2019) Changes in synaptic proteins precede neurodegeneration markers in preclinical Alzheimer's disease cerebrospinal fluid*. Mol Cell Proteomics 18:546–560. https://doi.org/10.1074/mcp.RA118.001290
4. Selkoe DJ (1979) (2002) Alzheimer's disease is a synaptic failure. Science 298:789–791
5. Camporesi E, Nilsson J, Brinkmalm A, Becker B, Ashton NJ, Blennow K, Zetterberg H (2020) Fluid Biomarkers for Synaptic Dysfunction and Loss. Biomark Insights 15:1177271920950319. https://doi.org/10.1177/1177271920950319. PMID: 32913390; PMCID: PMC7444114
6. Milà-Alomà M, Brinkmalm A, Ashton NJ et al (2021) CSF Synaptic Biomarkers in the Preclinical Stage of Alzheimer Disease and Their Association With MRI and PET. Neurology 97:e2065. https://doi.org/10.1212/WNL.0000000000012853
7. de San G, José N, Massa F, Halbgebauer S et al (2022) Neuronal pentraxins as biomarkers of synaptic activity: from physiological functions to pathological changes in neurodegeneration. J Neural Transm 129:207–230
8. Llano DA, Devanarayan P, Devanarayan V (2023) CSF peptides from VGF and other markers enhance prediction of MCI to AD progression using the ATN framework. Neurobiol Aging 121:15–27. https://doi.org/10.1016/j.neurobiolaging.2022.07.015
9. Sathe G, Albert M, Darrow J et al (2021) Quantitative proteomic analysis of the frontal cortex in Alzheimer's disease. J Neurochem 156:988–1002. https://doi.org/10.1111/jnc.15116
10. Nilsson J, Gobom J, Sjödin S et al (2021) Cerebrospinal fluid biomarker panel for synaptic dysfunction in alzheimer's disease. Alzheimer's Dem Diag Assess Dis Mon. https://doi.org/10.1002/dad2.12179
11. Libiger O, Shaw LM, Watson MH et al (2021) Longitudinal CSF proteomics identifies NPTX2 as a prognostic biomarker of Alzheimer's disease. Alzheimer's Dem 17:1976–1987. https://doi.org/10.1002/alz.12353
12. Soldan A, Oh S, Ryu T et al (2023) NPTX2 in Cerebrospinal Fluid Predicts the Progression From Normal Cognition to Mild Cognitive Impairment. Ann Neurol. https://doi.org/10.1002/ana.26725
13. Xiao M-F, Xu D, Craig MT et al (2017) NPTX2 and cognitive dysfunction in Alzheimer's Disease. Elife. https://doi.org/10.7554/eLife.23798
14. Watson CM, Dammer EB, Ping L et al (2023) Quantitative Mass Spectrometry Analysis of Cerebrospinal Fluid Protein Biomarkers in Alzheimer's Disease. Sci Data 10:261. https://doi.org/10.1038/s41597-023-02158-3
15. Perna A, Marathe S, Dreos R et al (2021) Revealing NOTCH-dependencies in synaptic targets associated with Alzheimer's disease. Mol Cell Neurosci. https://doi.org/10.1016/j.mcn.2021.103657
16. Portelius E, Zetterberg H, Skillbäck T et al (2015) Cerebrospinal fluid neurogranin: Relation to cognition and neurodegeneration in Alzheimer's disease. Brain 138:3373–3385. https://doi.org/10.1093/brain/awv267
17. Massa F, Halbgebauer S, Barba L et al (2022) Exploring the brain metabolic correlates of process-specific CSF biomarkers in patients with MCI due to Alzheimer's disease: preliminary data. Neurobiol Aging 117:212–221
18. Albert MS, DeKosky ST, Dickson D et al (2011) The diagnosis of mild cognitive impairment due to Alzheimer's disease: Recommendations from the National Institute on Aging-Alzheimer's Association workgroups on diagnostic guidelines for Alzheimer's disease. Alzheimer's Dem 7:270–279. https://doi.org/10.1016/j.jalz.2011.03.008
19. Jack CR, Bennett DA, Blennow K et al (2018) NIA-AA Research Framework: Toward a biological definition of Alzheimer's disease. Alzheimer's and Dementia 14:535–562
20. Petersen RC, Caracciolo B, Brayne C et al (2014) Mild cognitive impairment: a concept in evolution. J Intern Med 275:214–228. https://doi.org/10.1111/joim.12190
21. Aisen PS, Petersen RC, Donohue MC et al (2010) Clinical core of the Alzheimer's disease neuroimaging initiative: Progress and plans. Alzheimer's and Dementia 6:239–246. https://doi.org/10.1016/j.jalz.2010.03.006
22. Edmonds EC, McDonald CR, Marshall A et al (2019) Early versus late MCI: Improved MCI staging using a neuropsychological approach. Alzheimer's Dem 15:699–708. https://doi.org/10.1016/j.jalz.2018.12.009
23. Soldan A, Moghekar A, Walker KA et al (2019) Resting-state functional connectivity is associated with cerebrospinal fluid levels of the synaptic protein NPTX2 in non-demented older adults. Front Aging Neurosci. https://doi.org/10.3389/fnagi.2019.00132
24. Galasko D, Xiao M, Xu D et al (2019) Synaptic biomarkers in CSF aid in diagnosis, correlate with cognition and predict progression in MCI and Alzheimer's disease. Alzheimer's Dem Translat Res Clin Intervent 5:871–882. https://doi.org/10.1016/j.trci.2019.11.002
25. Saura CA, Parra-Damas A, Enriquez-Barreto L (2015) Gene expression parallels synaptic excitability and plasticity changes in Alzheimer's disease. Front Cell Neurosci 9:318. https://doi.org/10.3389/fncel.2015.00318. PMID: 26379494; PMCID: PMC4548151
26. Duits FH, Brinkmalm G, Teunissen CE et al (2018) Synaptic proteins in CSF as potential novel biomarkers for prognosis in prodromal Alzheimer's disease. Alzheimers Res Ther. https://doi.org/10.1186/s13195-017-0335-x
27. DeKosky ST, Scheff SW (1990) Synapse loss in frontal cortex biopsies in Alzheimer's disease: Correlation with cognitive severity. Ann Neurol 27:457–464
28. Scheff SW, DeKosky ST, Price DA (1990) Quantitative assessment of cortical synaptic density in Alzheimer's disease. Neurobiol Aging 11:29–37

29. Kovács RA, Vadászi H, Bulyáki E et al (2021) Identification of Neuronal Pentraxins as Synaptic Binding Partners of C1q and the Involvement of NP1 in Synaptic Pruning in Adult Mice. Front Immunol. https://doi.org/10.3389/fimmu.2020.599771
30. Swanson A, Willette AA (2016) Neuronal Pentraxin 2 predicts medial temporal atrophy and memory decline across the Alzheimer's disease spectrum. Brain Behav Immun 58:201–208. https://doi.org/10.1016/j.bbi.2016.07.148
31. Zhou J, Wade SD, Graykowski D et al (2023) The neuronal pentraxin Nptx2 regulates complement activity and restrains microglia-mediated synapse loss in neurodegeneration. Sci Transl Med. https://doi.org/10.1126/scitranslmed.adf0141
32. Nobili F, Schmidt R, Carriò I, Frisoni GB (2018) Brain FDG-PET: clinical use in dementing neurodegenerative conditions. Eur J Nucl Med Mol Imaging 45:1467–1469
33. Provost K, La Joie R, Strom A et al (2021) Crossed cerebellar diaschisis on 18F-FDG PET: Frequency across neurodegenerative syndromes and association with 11C-PIB and 18F-Flortaucipir. J Cereb Blood Flow Metab 41:2329–2343. https://doi.org/10.1177/0271678X211001216
34. Zimmer ER, Parent MJ, Souza DG et al (2017) [18F]FDG PET signal is driven by astroglial glutamate transport. Nat Neurosci 20:393–395. https://doi.org/10.1038/nn.4492
35. Nakashima T, Nakayama N, Miwa K et al (2007) Focal Brain Glucose Hypometabolism in Patients with Neuropsychologic Deficits after Diffuse Axonal Injury. Am J Neuroradiol 28:236
36. Herholz K (2003) PET studies in dementia. Ann Nucl Med 17:79–89. https://doi.org/10.1007/BF02988444
37. Soonawala D, Amin T, Ebmeier KP et al (2002) Statistical parametric mapping of 99mTc-HMPAO-SPECT images for the diagnosis of Alzheimer's disease: Normalizing to cerebellar tracer uptake. Neuroimage 17:1193–1202. https://doi.org/10.1006/nimg.2002.1259
38. Matsuda H (2001) Cerebral blood flow and metabolic abnormalities in Alzheimer's disease. Ann Nucl Med 15:85–92. https://doi.org/10.1007/BF02988596
39. Belbin O, Xiao MF, Xu D et al (2020) Cerebrospinal fluid profile of NPTX2 supports role of Alzheimer's disease-related inhibitory circuit dysfunction in adults with down syndrome. Mol Neurodegener 15:1–10. https://doi.org/10.1186/s13024-020-00398-0

Springer Nature or its licensor (e.g. a society or other partner) holds exclusive rights to this article under a publishing agreement with the author(s) or other rightsholder(s); author self-archiving of the accepted manuscript version of this article is solely governed by the terms of such publishing agreement and applicable law.